Natural convection in a square cavity with two baffles on the vertical walls: experimental and numerical investigation

Giorgia Nardini, Massimo Paroncini, and Raffaella Vitali

***Abstract*—**Natural convection in a square enclosure filled with air is experimentally and numerically analyzed. The cavity has horizontal and vertical Plexiglas walls with discrete sources. Two Plexiglas baffles are attached to its vertical walls between the sources symmetrically. The effect of different baffle lengths is investigated. The results are presented for Rayleigh numbers from 10^4 to 10^5. The fluid flow field, thermal field and heat transfer are analyzed for two different baffle lengths through interferograms, streamlines, isotherms and velocity maps. The dimensionless baffle lengths investigated are L_b= 0.2 and L_b= 0.4.

The results clearly demonstrate that different baffle lengths have a significant effect on the heat transfer and flow characteristics of the fluid. The flow field pattern is baffle length and Rayleigh number dependent. It is, in fact, observed that for L_b= 0.2 the flow tends to circulate as a vortex strangled by the baffles, while for L_b= 0.4 the flow tends to separate into two different vortices. The Nusselt number increases as Rayleigh number increases and it is a decreasing function of baffle length for the lower sources and increases for the higher sources.

The average Nusselt numbers from L_b = 0.2 to L_b = 0.4 decrease on average by 23% on the lower source and it increases on average by 29% on the higher source.

***Keywords*—**Baffles, Holographic Interferometry,Natural Convection, Square Cavity.

I. Introduction

NATURAL document convection heat transfer in an air filled cavity has received great attention because many industrial applications employ this concept as a prototype. Noticeable examples include heating and ventilating of rooms, insulation with double-pane windows, solar collector systems and the cooling of electronic equipment. In many engineering applications, the cavity is portioned by baffle(s) attached to its vertical or horizontal wall(s). A review of the recent literature finds that both the size and position of the baffle(s) have a significant effect on natural convective heat transfer and flow characteristics of the fluid. Studies of this problem are carried out by many researchers theoretically, numerically and experimentally. The baffle(s) can be attached to the vertical wall(s) or to the horizontal wall(s). Regarding the baffle attached to the vertical wall, Bajorek and Lloyd [1] experimentally analysed a differentially heated air filled square cavity with an insulated baffle with dimensionless length of 0.25 positioned in the middle of the horizontal wall. The vertical walls were maintained isothermal at different temperatures, while the horizontal walls and partitions were insulated. Jetli et al. [2] numerically studied a differentially heated, air filled, square partitioned enclosure with two offset baffles and perfectly conducting horizontal end walls. Three different baffle locations of dimensionless length, fixed at 0.33 were investigated. Ambarita et al. [3] numerically investigated laminar natural convective heat transfer in a differentially heated, square cavity with isothermal left and right walls at T_h and T_c respectively (T_h>T_c); the horizontal walls were adiabatic. Two insulated baffles were attached to the horizontal walls at symmetric positions and the dimensionless baffle lengths examined were 0.6, 0.7, and 0.8.

Concerning the baffle attached to the horizontal wall, Bilgen [4] carried out a numerical study of natural convection in a differentially heated, square cavity with the left isothermal wall at Th and the right at Tc with insulated horizontal walls. A thin fin is attached to the hot wall with dimensionless fin length from 0.10 to 0.90. Facas [5] presented numerical calculations for the natural convective flow inside an air-filled cavity with fins/baffles - of length 0.1, 0.3, and 0.5 of the cavity width - attached along both the heated and the cooled side of the cavity. Ghassemi at al. [6] numerically investigated the effect of two insulated horizontal baffles- of dimensionless length 0.5, 0.6, 0.7, and 0.8 placed at different positions of the walls of a differentially heated square cavity with left and right isothermal walls at T_h and T_c respectively (T_h>T_c) and adiabatic horizontal walls. Other numerical investigations were carried out, for example, by Tasnim and Collins [7], Frederick [8], Yamaguchi and Asako [9], Nag et al. [10] and Shi and Khodadadi [11].

However there are few experimental contributions regarding cavities with baffle(s).

In this paper we will experimentally and numerically analyze a square cavity of side length H with four discrete sources of height H/4 (two hot sources kept at a temperature T_h that changes from one test to another to obtain different Rayleigh numbers and two cold sources maintained at a fixed

G.Nardini is with the DIISM, Dipartimento di IngegneriaIndustriale e ScienzeMatematiche, UniversitàPolitecnicadelle Marche, Via BrecceBianche - 60131 Ancona, ITALY (corresponding author phone +390712204876, fax +390712204770, e-mail: g.nardini@univpm.it).

M.Paroncini., is with the DIISM, Dipartimento di IngegneriaIndustriale e ScienzeMatematiche, UniversitàPolitecnicadelle Marche, Via BrecceBianche - 60131 Ancona, ITALY (e-mail: m.paroncini@univpm.it).

R.Vitali is with the DIISM, Dipartimento di IngegneriaIndustriale e ScienzeMatematiche, UniversitàPolitecnicadelle Marche, Via BrecceBianche - 60131 Ancona, ITALY (e-mail: r.vitali@univpm.it).

temperature T_c) located on the vertical walls with two baffles attached in the middle of the vertical walls between the sources in symmetric positions. The baffles are in Plexiglas, an isolating material, with a dimensionless height of 0.18 and dimensionless length from 0.2 to 0.4. The purpose of this paper is to clarify the effects of the baffles' length on the flow and temperature fields and on the heat transfer characteristics of the cavity. The thermal behavior of heat transfer is experimentally studied through holographic interferometry. The experimental and numerical correlations between the Rayleigh numbers and corresponding Nusselt numbers are analyzed.

NOMENCLATURE

a = Thermal diffusivity [m^2s^{-1}]
g = Modulus of the gravity vector [ms^{-2}]
k = Thermal conductivity [$Wm^{-1}K^{-1}$]
H = Height cavity side [m]
Y_b = dimensionless height of baffle, h_b/H
L_b = dimensionless length of baffle, l_b/H
h_b = baffle height [m]
l_b = baffle length [m]
l = Heat source length [m]
L = Cavity width in the experimental tests [m]
Nu_h = Local Nusselt number of the heat source
Nu_{ave} = Average Nusselt number of the heat source
Nu_{higher}= Average Nusselt number of the higher heat source
Nu_{lower} = Average Nusselt number of the lower heat source
Pr = Prandlt number
Ra = Rayleigh number
T = Temperature [K]
ΔT = Temperature difference between heat sources and cold strips
x = Cartesian axis direction
X = Dimensionless Cartesian axis direction
y = Cartesian axis direction
Y = Dimensionless Cartesian axis direction

Greek symbols

β = Thermal expansion coefficient [K^{-1}]
ε = Dimensionless length of the heat source
θ = Dimensionless temperature
ρ = Density [kgm^{-3}]
υ = Kinematic viscosity [m^2s^{-1}]

Subscripts

c = Cold wall
cal= Calculated data
exp = Experimental data
h = Hot wall
num = Numerical data

II. Materials and Methods

A. Experimental Analysis

1) Experimental Setting

The square cavity has side length H of 0.05 m and it has four sources of height H/4 located on its vertical walls. The cavity is a square transversal section whose length in the longitudinal direction (L = 8.1H) that is much greater than H, allowing the motion develop along the z axis, parallel to the laser beam, with a two-dimensional shape. Two baffles are attached to its vertical walls between two sources in symmetric position. The Plexiglas baffles' dimensions are: Y_b is 0.18 and L_b varies from 0.2 to 0.4. A scheme of the cavity and its coordinate system are shown in Fig.1.

Cold sources are maintained at a fixed temperature T_c (291.16 K), and heat sources are kept at a temperature T_h that change from one test to another to obtain different Rayleigh numbers. The heat sources are an aluminum pipe with a rectangular transversal section, flush mounted on the lateral walls of the cavity. The cavity surfaces are in Plexiglas to prevent heat leakage through the walls. The vertical walls are crossed by four aluminum channels connected to two thermostatic baths, which provide the circulation of the heating and cooling fluid that maintain the strips at temperatures of T_c and T_h.

2) Holographic Interferometry

The experimental set up is composed of a test cell, which is filled with air at atmospheric pressure, a thermal system (two thermostatic baths, the thermal circuit and the temperature control system), a pneumatic auto-leveling table, a laser source, all of the necessary optical instrumentation and an acquisition system (see Fig.2).

The cavity is filled with air (Pr = 0.71) at atmospheric pressure, a room temperature of 295 K and a relative humidity of 50 %.

The thermostatic circuit is composed of two thermostats with their respective connecting pipes. The PROLINE RP1840 and RC20 thermostats are manufactured by Lauda Company. Each pipe that connects the thermostats with the inlet and outlet valves of the two sidewalls and the heater is covered with a neoprene skin (approximately 0.02 m thick) to insulate it, preventing heat loss. The thermostatic fluid is a mixture of 75 % water and 25 % glycol.

The acquisition system is composed of thirteen copper-constantan thermocouples located 1 mm under the surface of the test volume and are fixed through conductive paste. Three thermocouples are inserted along the middle axis to measure the surface temperatures in each source.

The thermocouples are connected to an ice point reference manufactured by Kaye, model K170. Unfortunately, these temperatures cannot be used directly to obtain the temperature distribution of the fringes during the interpretation of the interferograms because, due to the effects of diffraction, the positions of both the heater and sidewalls are uncertain. For this reason, the last thermocouple is positioned in the middle of the air region to provide a reference temperature for the analysis of the interferograms. The laser used is a ''Model 532-400 DPSS'', diode-pumped, frequency-doubled Nd:YAG laser that emits an output beam at a 532 nm (green) wavelength.

The analysis of the convective heat transfer phenomenon is conducted with the real-time and double-exposure technique.

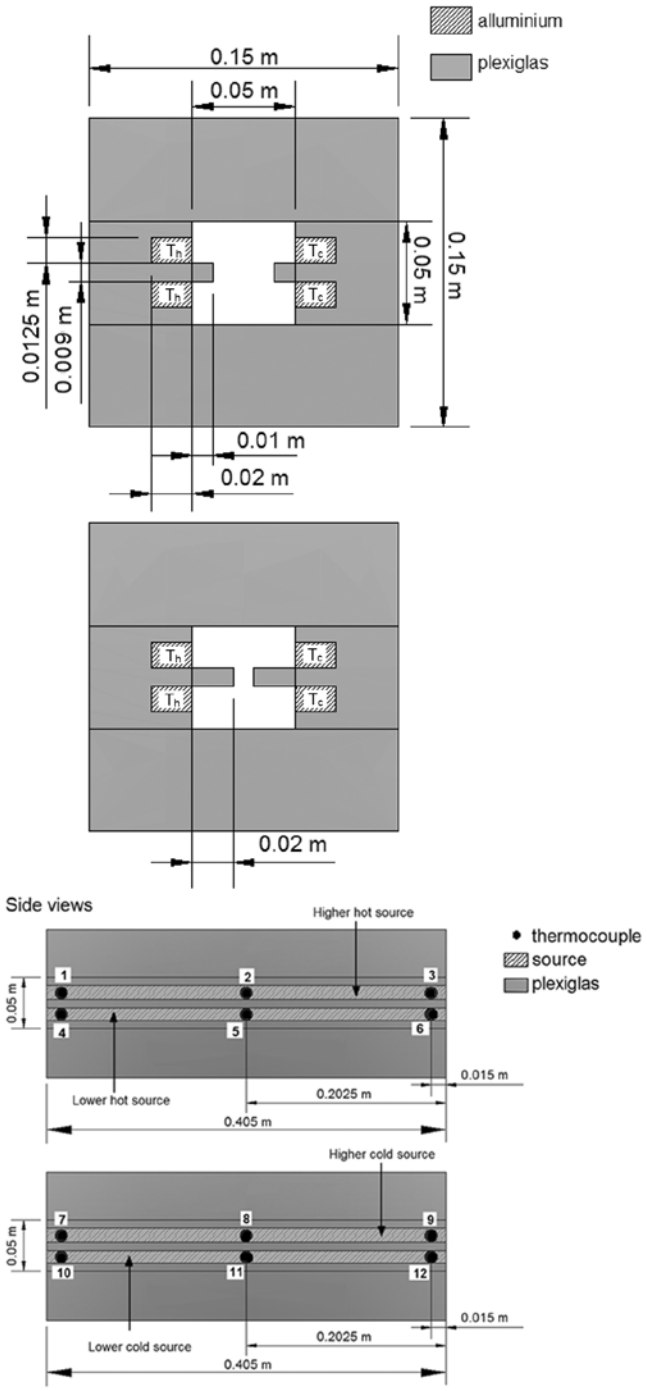

Fig.1 Top: cavity design with baffle L_b = 0.2. Middle: cavity design with baffle L_b = 0.4. Bottom: Side views of the cavities with thermocouple positions along the Higher and Lower sources. The position of the 13th thermocouple, located in the center of the cavity may be seen in Fig.3 and Fig. 4.

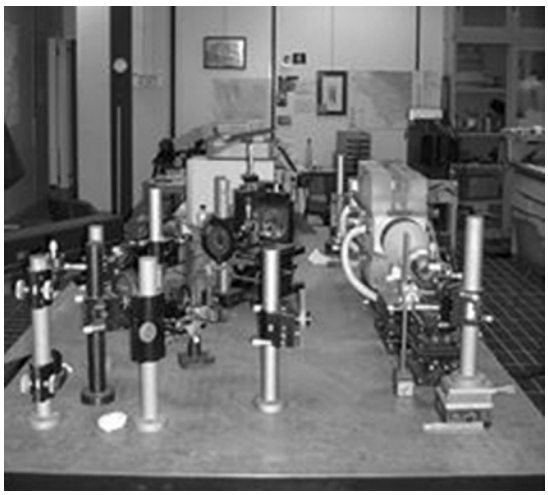

Fig.2 The holographic interferometry setup

The real-time technique is used in order to reveal the presence of plume oscillations to study the temporal evolution of the transfer processes, while the double-exposure technique is used for steady-state measurements. Holographic interferometry shows the typical advantages over the classical optical techniques, such as high precision and sensitivity, very low noise level, and the possibility of displaying the temperature distribution across the whole investigated region. The interferograms are analyzed with a traveling microscope to obtain the intensity distribution.

The density and temperature distributions are obtained by the usual methods of inversion. According to Hauf and Grigull [12], the expected accuracy for small fringe numbers (less than 30) can be approximately 10 %.

B. Numerical Analysis

Fluent solution methods are known in the scientific background. In this study, the numerical simulation is developed using the finite volume code Fluent 12.1.4 using the Boussinesq approximation for air and is performed with a 2d double precision approximation.

1) Segregated Solver

The numerical results are carried out through the segregated solvers [13] for Rayleigh number from10^4 to 10^5, and they are compared with the experimental data. In this study, a second order upwind implicit scheme is employed for the momentum and energy equations. The pressure interpolation is provided by the Body Force Weighted scheme; the pressure velocity coupling is provided by the SIMPLE algorithm, and a two-dimensional model is used with the condition of laminar flow. The diffusion terms are central-differenced with a second order accuracy.

2) Numerical Settings

The entire test cell (cavity + Plexiglas walls) is reproduced with real dimensions, so the computational domain coincides with the entire cavity as seen in Fig. 1. A non-uniform mesh was employed: a dense uniform quadrilateral mesh covers the cavity where the solution needs to be most accurate, while a sparse mesh covers the Plexiglas walls of the cavity. A preliminary study to identify the lowest number of cells

necessary to obtain results that were independent of the number of cells was carried out. The total number of cells for both configurations is 399136.

The temperatures of the heated strips are assigned in order to obtain the analyzed Rayleigh numbers as in the experimental analysis. The top and the bottom surfaces take into account the conductive heat flux through the Plexiglas walls. The Plexiglas element is introduced in the Fluent model. It is necessary to simulate the conductive heat transfer between these elements using the conjugate heat transfer.

The cold sources are kept at a constant temperature of 291.16K for all the simulations, while the hot sources are kept at a constant temperature during the single simulation but the temperature varies for each simulation. In order to simulate the non-adiabatic nature of the Plexiglas, convection with a constant heat convection coefficient of 8 $Wm^{-2}K^{-1}$ and a free stream temperature of 291K are the boundary conditions on the external Plexiglas walls. The boundary conditions at the internal Plexiglas – air interface are coupled.

3) Simulation Procedure

The numerical average Nusselt numbers (Nu_{ave}) on the heating elements are given by

$$\overline{Nu} = \frac{q_{tot}/A_h}{k \cdot \Delta T/H} \quad (1)$$

where q_{tot} is the heat transfer rate directly computed by Fluent, A_h is the heater surface that is considered, and k is the thermal conductivity of the air evaluated at the heating strips temperature.

The local Nusselt numbers (Nu_h) are also referred to the heat sources, and they are calculated as

$$Nu_h = \frac{q''}{k \cdot \Delta T/H} \quad (2)$$

where q" is the heat flux computed by Fluent on each cell of the mesh.

III. Results and Discussion

Geometrical and thermal parameters governing the heat transfer in the square cavity with four discrete sources with two baffles attached to its vertical walls in symmetric position are: side length of cavity H, height sources H/4, the height of baffles Y_b = 0.18 and the dimensionless length of the baffles L_b varies from 0.2 to 0.4. Rayleigh number varies from 10^4 to 10^5 and the fluid inside cavity is dry air with Pr = 0.71. Flow and temperature fields and heat transfer in the cavity are analyzed.

A. Flow and Temperature Fields

Some examples of experimental and numerical flow and temperature fields for L_b = 0.2 and L_b = 0.4 are presented in Fig. 3, 4, 5, and 6. The figures are arranged going from left to right with the ascending Ra numbers.

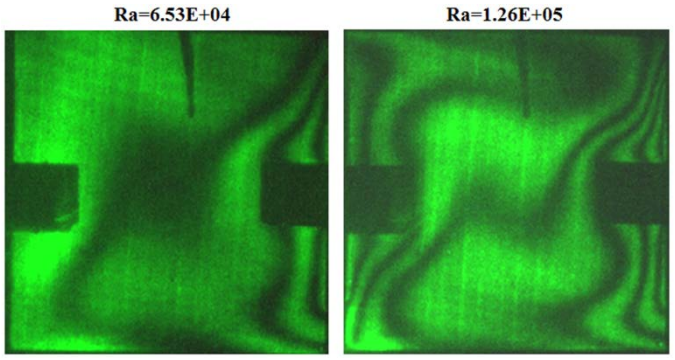

Fig.3 Examples of the interferograms for L_b = 0.2

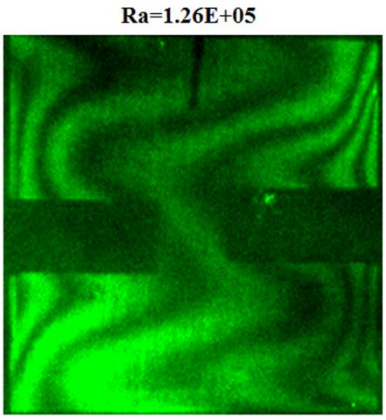

Fig. 4 Example of the interferograms for Lb = 0.4

Examining Fig. 3, 4, 5 and 6 it is possible to note that the fringes in the upper and lower portion of the cavity are not perpendicular to the horizontal surface, showing that the top and the bottom of the enclosure is not perfectly adiabatic. The different lengths of the two baffles inside the cavity totally modify the flow field patterns. In fact for L_b = 0.2 the fluid circulates and creates a large clockwise primary vortex strangled by the baffles while for L_b = 0.4 the fluid is separated into two different vortexes and the two baffles create a fluid trapping phenomena in the cavity. For low Rayleigh numbers, $Ra=10^4$, natural convection is weak for both L_b lengths but the space between the baffles for L_b = 0.4 is smaller compared to the corresponding case for L_b= 0.2 so the primary vortex is divided into two vortices when L_b varies from 0.2 to 0.4. For L_b = 0.4 there are two trapped fluids in the cavity, the bottom trapped fluid and top trapped fluid. The bottom trapped fluid exists between the baffles and bottom wall and top trapped fluid exists between the baffles and top wall. These trapped fluids create two vortices one shifted towards the top wall above the baffles and the other one shifted towards the bottom cavity wall, under the baffles. This is because natural convection is more vigorous in the top and bottom of the cavity. These two vortices are separated by the trapped fluid which is stagnant between the two baffles.

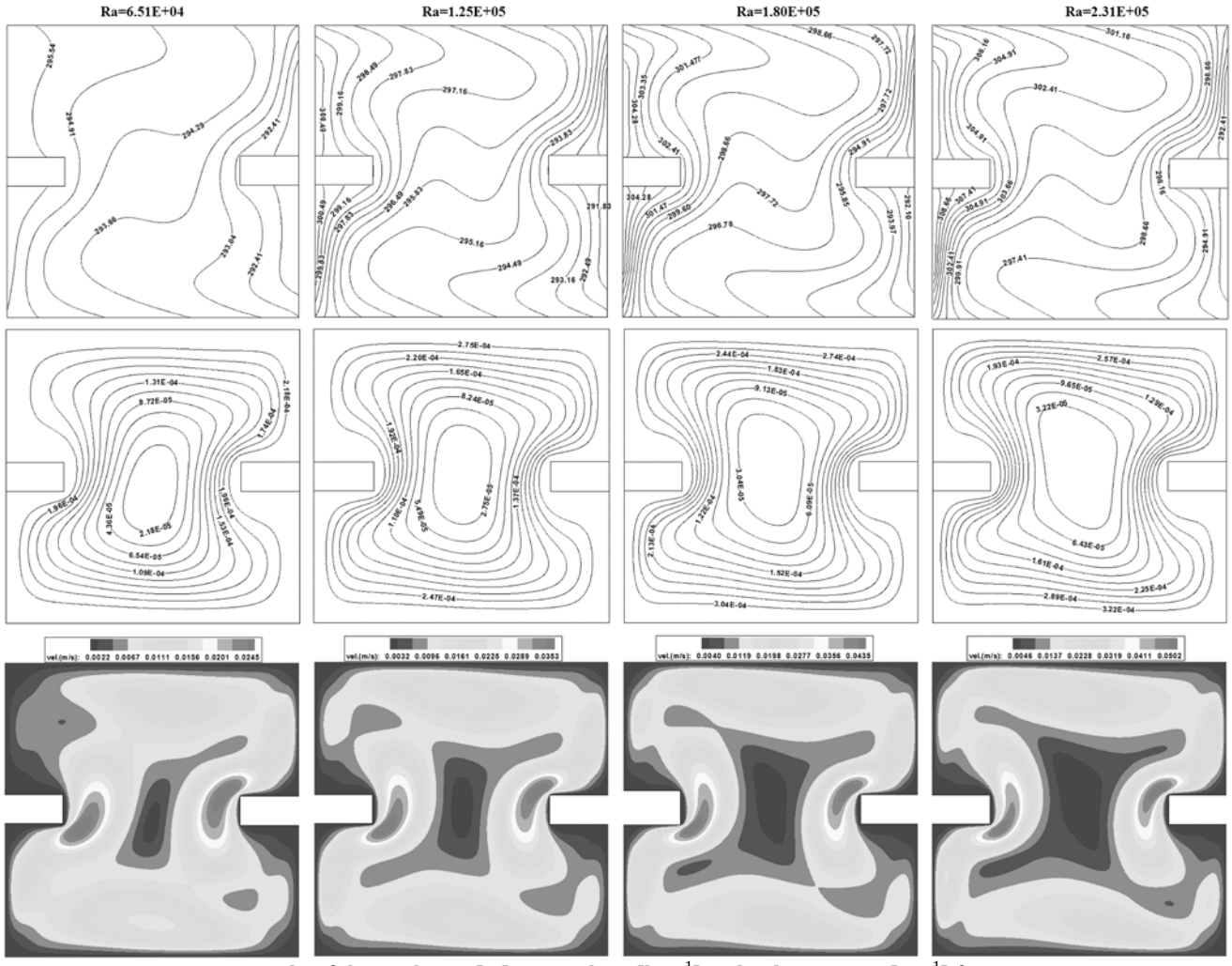

Fig. 5Example of the isotherms[K], streamlines[kgs^{-1}] and velocity maps[ms^{-1}] for $L_b = 0.2$

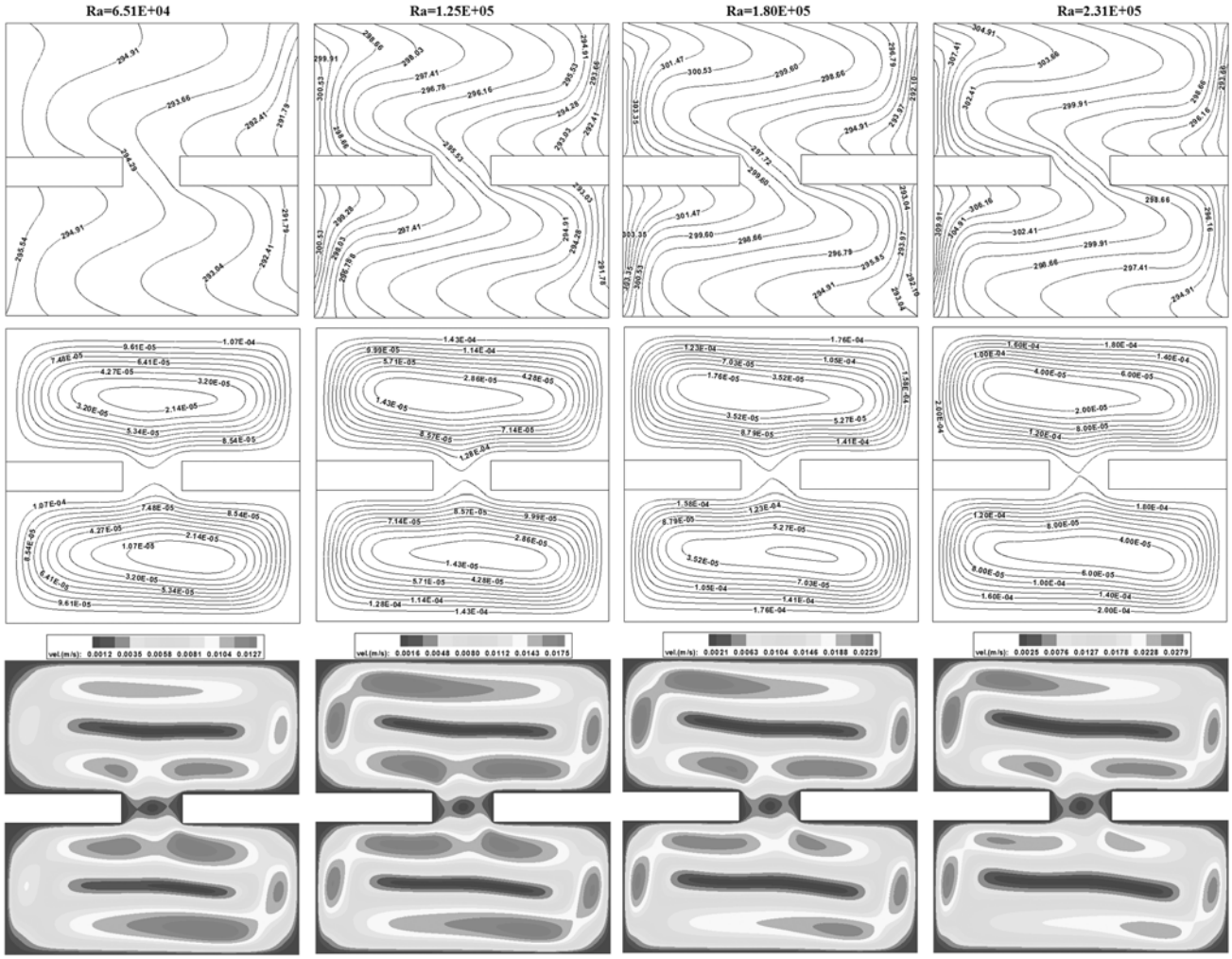

Fig. 6 Example of the isotherms[K], streamlines[kgs^{-1}] and velocity maps[ms^{-1}] for L_b = 0.4

For L_b = 0.2 at low Ra, a weak vortex is formed between two baffles and by increasing Ra this vortex will be strengthened.

The trapped fluid, for both configurations, can be seen clearly at Ra=10^5, this is because the vortex for L_b = 0.2 and the vortices for L_b = 0.4 become more vigorous as seen by the increasingly packed streamlines (Fig. 5 and Fig. 6). At Ra=10^5 for L_b = 0.2 and L_b = 0.4 the isotherms at the top and bottom of the cavity become almost vertical between the two baffles and insulated walls. This is because natural convection is more vigorous in the top and bottom portions of the cavity.

Another feature of these temperature patterns is that the streamlines become more packed next to the sidewall as the Ra increases for both L_b values. This suggests that the flow moves faster as natural convection intensifies. The maximum absolute value of the stream function can be viewed as a measure of the intensity of natural convection in the cavity. As the Ra increases, the maximum absolute value of the stream function increases.

B. Heat transfer

In order to understand the effect of baffle length, the average Nusselt numbers will be discussed. The experimental and numerical average Nusselt numbers for L_b = 0.2 and L_b = 0.4 as a function of Rayleigh number are shown in Tables I and II, for Ra numbers that vary from 10^4 to 10^5.

The Rayleigh numbers are defined as:

$$Ra = \frac{(g \cdot \beta \cdot (T_h - T_c) \cdot H^3)}{\nu \cdot a} \tag{3}$$

The dimensionless parameters used are:

$$X = \frac{x}{H}; Y = \frac{y}{H}; \theta = \frac{(T - T_c)}{(T_h - T_c)}; \varepsilon = \frac{l}{H} \tag{4}$$

The local Nusselt number – Nu(Y) –on the hot sources is calculated employing the expression:

$$Nu_h(Y) = -\left.\frac{\partial \theta}{\partial X}\right|_{X=0} \tag{5}$$

The average Nusselt number - Nu_{ave} - on the heat sources is given by the relation:

$$Nu_{ave} = \frac{1}{\varepsilon}\int_0^{\varepsilon} Nu_h(Y)dY \tag{6}$$

The height of the higher hot source is evenly divided into parts, taking into account the scale factor and the temperature profile. For each of these parts, the local Nusselt number is calculated applying (5). Once the local Nusselt numbers for

the strip are determined, (6) is applied to obtain the average Nusselt number for the higher hot source (Nu_{higher}). The aforementioned procedure is repeated for the lower hot source in order to obtain the average Nusselt number for the strip (Nu_{lower}). The heat transfer rate for each hot source across the entire cavity is described by the average Nusselt number.

Table I Experimental Nusselt numbers for L_b = 0.2, L_b = 0.4

L_b = 0.2			L_b = 0.4		
Rayleigh Number	Higher source	Lower source	Rayleigh Number	Higher source	Lower source
Ra	Nu	Nu	Ra	Nu	Nu
6.53E+04	1.21	2.74	6.54E+04	1.63	1.87
7.83E+04	1.26	3.14	7.82E+04	1.93	2.42
9.16E+04	1.42	3.54	9.15E+04	2.24	2.80
1.26E+05	2.21	4.58	1.26E+05	2.27	3.90
1.40E+05	2.28	4.88	1.41E+05	3.40	4.18
1.62E+05	2.36	5.46	1.61E+05	3.86	4.73
1.82E+05	2.43	5.87	1.81E+05	4.31	4.88
2.35E+05	2.96	7.24	2.34E+05	5.51	6.69

Table II Numerical Nusselt numbers for L_b = 0.2 and L_b = 0.4

L_b = 0.2			L_b = 0.4		
Rayleigh Number	Higher source	Lower source	Rayleigh Number	Higher source	Lower source
Ra	Nu	Nu	Ra	Nu	Nu
6.51E+04	1.33	2.7	6.51E+04	1.74	1.84
1.25E+05	2.36	4.73	1.25E+05	3.35	3.74
1.80E+05	2.94	5.82	1.80E+05	4.21	4.79
2.31E+05	3.35	6.58	2.31E+05	4.81	5.52
2.78E+05	3.67	7.17	2.78E+05	5.26	6.07
3.22E+05	3.93	7.65	3.22E+05	5.62	6.52
3.98E+05	4.30	8.36	3.98E+05	6.14	7.18

Observing Tables I and II it is possible to see a good qualitative agreement between the numerical and the experimental temperature distribution in the cavity for both L_b = 0.2 and for L_b = 0.4. In fact the differences between the experimental and numerical Nusselt numbers for L_b = 0.2 are less than -6.78 % on the higher source and 3.27% on the lower source while the difference between the experimental and numerical Nusselt numbers for L_b = 0.4 are less than -11.51% on the higher source and 4.10% on the lower source. In particular, the worst result (-11.51%) is recorded for Ra=$6.54 \cdot 10^4$.

As shown in Tables I and II, the Nusselt number is an increasing function of Ra and baffle length dependent. Observing Tables I and II the lower source always has the higher heat transfer coefficient. This fact is due to the upward moving plume from the lower source that impinges on the higher source and affects its heat transfer characteristics. The fact that the fluid arriving at the higher source is in motion means that the higher source is situated in what appears to be forced convection flow. On the other hand, the heat transfer at the lower source tends to increase the temperature of the fluid that reaches the higher source with a value that is higher than the one of the ambient fluid. Consequently the buoyancy plume from the lower source decreases the heat flux of the higher source. This phenomenon is reduced by increasing the baffle length as shown by the Nusselt numbers on the higher sources that are higher when L_b =0.4 than the values for L_b=0.2. When L_b=0.4 the higher source is less affected by the buoyancy plume from the lower source and so the heat flux on the higher source increases. The numerical average Nusselt numbers as a function of Rayleigh number for L_b=0.2 and L_b=0.4 are presented in Fig.7.

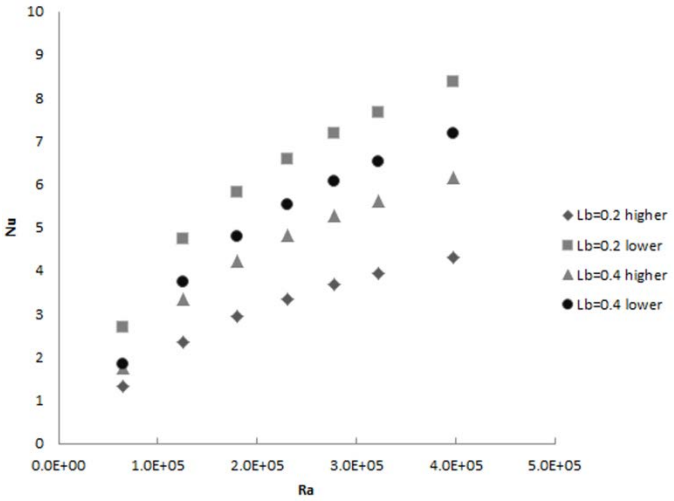

Fig.7 Numerical Nusselt numbers for L_b = 0.2 and L_b = 0.4

As shown in Fig.7 different baffle lengths modify the flow, temperature fields and heat transfer characteristics of the cavity.In fact from L_b = 0.2 to L_b = 0.4 the average Nusselt number decreases on average by 24% at the lower source with a minimum value of 16% for Ra = $3.98 \cdot 10^5$ and a maximum value of 47% for Ra = $6.51 \cdot 10^4$, while the average Nusselt number increases on average by 29% at the higher source with a minimum value of 24% for Ra = $6.51 \cdot 10^4$ and a maximum value of 30% for Ra = $2.78 \cdot 10^5$.

These values suggest that baffle length has a significant effect on the heat transfer and flow characteristics of the fluid.

A relation between the average Nusselt numbers and the corresponding Rayleigh numbers is also elaborated.
This relation is:

$$Nu_{cal} = a \cdot Ra^b \tag{7}$$

The values of the parameters and the correlation coefficients R^2 of (8) are shown in Tables III and IV.

R^2 is an indicator that describes the fitting of the function to the experimental data, and is defined as follows:

$$R^2 = 1 - \frac{SSE}{SST} \tag{8}$$

where

$$SST = (\sum_{j=1}^{n} k_j^{\,2}) + \frac{1}{n}(\sum_{j=1}^{n} k_j)^2 \tag{9}$$

and

$$SSE = \sum_{j=1}^{n} (k_j - h_j) \tag{10}$$

k_js are the n experimental values and h_js are the corresponding calculated value.

Table III Experimental and numerical correlation parameters

$L_b = 0.2$						
Experimental correlation parameters				Numerical correlation parameters		
	a	b	R^2	a	b	R^2
higher source	3.0E-04	0.75	0.95	1.2E-03	0.64	0.97
lower source	6.0E-04	0.75	0.99	3.2E-03	0.61	0.97

Table IV Experimental and numerical correlation parameters

$L_b = 0.4$						
Experimental correlation parameters				Numerical correlation parameters		
	a	b	R^2	a	b	R^2
higher source	4.0E-05	0.95	0.94	1.2E-03	0.64	0.97
lower source	5.0E-05	0.95	0.98	6.0E-04	0.73	0.96

IV. Conclusions

Heat transfer by natural convection in a square cavity with two insulated baffles is experimentally and numerically investigated. The cavity is composed of Plexiglas walls and four discrete sources in the vertical walls. Two Plexiglas baffles are attached to its vertical walls at symmetric position between the sources. Their dimensionless length, L_b, is varies from 0.2 to 0.4. The range of the Rayleigh number is from 10^4 to 10^5.

Two different flow field patterns are observed. The first pattern is a flow field with a large clockwise primary vortex strangled by the baffles, but increasing the baffle length causes a second pattern to be observed with two different vortices. The flow field pattern is dimensionless baffle length and Rayleigh number dependent. It is also observed that the lower source always has the higher heat transfer coefficient, Nusselt numbers increases as Rayleigh number increases and increasing the baffle length causes a decrease of 24% on average at the lower source while an average 29% increase is observed at the higher source.

Results obtained are useful for a better understanding of natural convection heat transfer in enclosures with discrete sources.

References

[1] S.M.Bajorek, and J.R. Lloyd, "Experimental investigation of natural convection in partitioned enclosures,"*J. Heat Transfer*, vol. 104,pp. 527-532, 1982.

[2] R.Jetli, S. Acharya, and E. Zimmerman, "Influence of the baffle location on natural convection in a partially divided enclosure,"*Numer. Heat Transfer*, vol. 10, pp. 521-536, 1986.

[3] H. Ambarita, K. Kishinami, M. Daimaruya, T. Saitoh, H. Takahashi, and J. Suzuki, "Laminar natural convection heat transfer in an air filled square cavity with two insulated baffles attached to its horizontal walls,"*Thermal Science & Engineering*, vol. 14, no.3, pp. 35-46, 2006.

[4] E. Bilgen, "Natural convection in cavities with a thin fin on the hot wall," *Int. J. Heat Mass Transfer*, vol. 48, pp. 3493-3505, 2005.

[5] G.N. Facas, "Natural convection in a cavity with fins attached to both vertical walls,"*J.Thermophys. Heat Transfer*, vol. 7, pp. 555-560, 1993.

[6] M.Gassemi, M. Pirmohammadi, and Gh.A. Sheikhzadeh, "A numerical study of natural convection in a cavity with two baffles attached to its vertical walls,"presented at the *5th IASME/WEAS Int. Conf. on Fluid Mechanics and Aerodynamics*, Athens, Grece, 2007, pp. 226-231.

[7] S.H. Tasnim, and M.R. Collins, "Numerical analysis of heat transfer in a square cavity with a baffle on the hot wall,"*Int. Commun. Heat Mass Transfer*, vol.31, pp. 639-650, 2004.

[8] R.L. Frederick, Natural convection in an inclined square enclosure with a partition attached to its cold wall,"*Int. J. Heat Mass Transfer*, vol.32, pp.87-94, 1989.

[9] Y. Yamaguchi, and Y. Asako, "Effects of partitions wall on natural convection heat transfer in a vertical air layer,"*J. Heat Transfer*, vol. 123, pp. 441-449, 2001.

[10] A. Nag, A. Sarkar, and V.M.K. Sastri, "Natural convection in a differentially heated square cavity with a horizontal partition plate on the hot wall,"*Comput. Meth Appl. Mech. Eng*., vol. 110, pp. 143–156, 1993.

[11] X. Shi, and J.M. Khodadadi, "Laminar convection heat transfer in a differentially heated square cavity due to a thin fin on the hot wall*J. Heat Transfer*, vol. 125,pp. 624–634, 2003.

[12] W. Hauf, and U. Grigull, "Optical methods in heat transfer," in*Advances in Heat transfer*, JP Harnett, TF Irvine Jr. (Eds), New York, Academic Press, 1970, pp. 133–311. doi:10.1016/S0065-2717(08) 70151-5

[13] "FLUENT User's Guide", Fluent Incorporated